Electron-Transfer Kinetics and Electric Double Layer Effects in Nanometer-Wide Thin-Layer Cells

Lixin Fan,[†] Yuwen Liu,[†] Jiewen Xiong,[‡] Henry S. White,[*,‡] and Shengli Chen[*,†]

[†]Hubei Key Laboratory of Electrochemical Power Sources, Key Laboratory of Analytical Chemistry for Biology and Medicine (Ministry of Education), Department of Chemistry, Wuhan University, Wuhan 430072, China, and [‡]Department of Chemistry, University of Utah, Salt Lake City, Utah 84112, United States

ABSTRACT Redox cycling in nanometer-wide thin-layer cells holds great promise in ultrasensitive voltammetric detection and in probing fast heterogeneous electron-transfer kinetics. Quantitative understanding of the influence of the nanometer gap distance on the redox processes in the thin-layer cells is of crucial importance for reliable data analysis. We present theoretical consideration on the voltammetric behaviors associated with redox cycling of electroactive molecules between two electrodes separated by nanometer widths. Emphasis is placed on the weakness of the commonly used Butler—Volmer theory and the classic Marcus—Hush theory in describing the electrochemical heterogeneous electron-transfer kinetics at potentials significantly removed from the formal potential of redox moieties and, in addition, the effect of the electric-double-layer on the electron-transfer kinetics and mass transport dynamics of charged redox species. The steady-state voltammetric responses, obtained by using the Butler—Volmer and Marcus—Hush models and that predicted by the more realistic electron-transfer kinetics formulism, which is based on the alignments of the density of states between the electrode continuum and the Gaussian distribution of redox agents, and by inclusion of the electric-double-layer effect, are compared through systematic finite element simulations. The effect of the gap width between the electrodes, the standard rate constant and reorganization energy for the electron-transfer reactions, and the charges of the redox moieties are considered. On the basis of the simulation results, the reliability of the conventional voltammetric analysis based on the Butler—Volmer kinetic model and diffusion transport equations is discussed for nanometer-wide thin-layer cells.

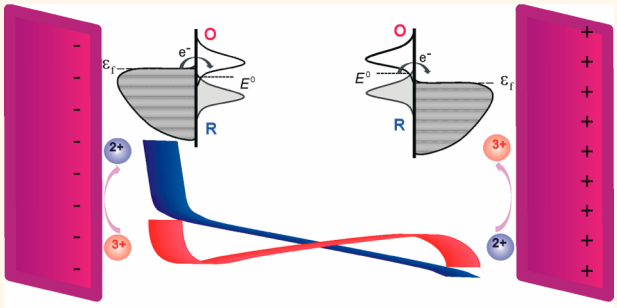

KEYWORDS: thin-layer cells · voltammetric responses · heterogeneous electron transfer · electric double layer · nanogap effects · finite element simulation

Redox cycling of dissolved electroactive species between two biased electrodes located in close proximity to each other can effectively increase the Faradaic current in electrochemical measurements.[1−6] The rate of the cycling, *i.e.*, amplification, increases in proportion to the inverse distance between two electrodes.[5,6] Nowadays, gap widths down to nanometer scales are achievable.[7−9] Nanofluidic thin-layer cells (NFTLCs) are typical examples. In addition to various novel sensing applications,[3,6,10,11] NFTLCs have been widely employed in fundamental electrochemical studies.[12−16] Particularly, they are among the most useful methods for studying the kinetics of the fast heterogeneous electron-transfer (ET) reactions under steady-state conditions, because they can efficiently overcome the mass transport (MT) limitations.[15,16]

In electrochemical studies using NFTLCs, the phenomenological Butler—Volmer (BV) theory has been frequently used to describe ET kinetics when performing voltammetric analysis. By assuming a linear relationship between the ET activation free energy and the electrode potential (E),[17] the BV model greatly facilitates the voltammetric analysis. It provides a satisfactory description of many electrochemical systems under usual experimental conditions. However, this linear-free-energy approximation may hold only if E is close to the formal potential (E^0) of the ET reaction. In electrode systems in which the MT rates are greatly enhanced, such that the ET kinetics-controlled voltammetric response extends to electrode

* Address correspondence to slchen@whu.edu.cn, white@chem.utah.edu.

Received for review July 10, 2014 and accepted September 11, 2014.

Published online September 11, 2014
10.1021/nn503780b

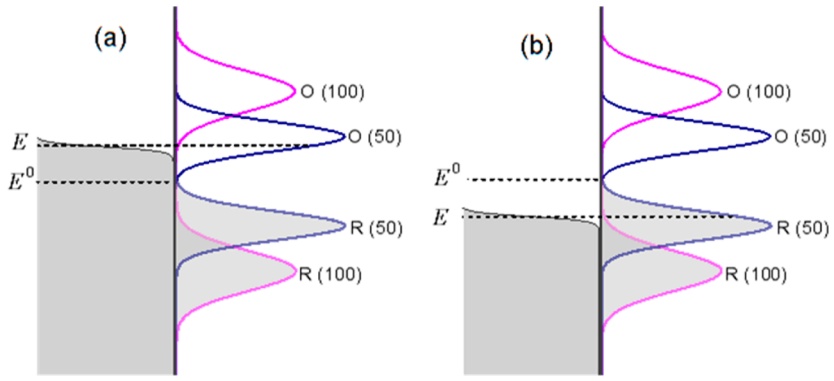

Figure 1. Schematic diagram of DOS overlap between the electrode and the redox couples of different reorganization energies (indicated by the values, kJ/mol, in the brackets), in the cases of reduction (panel a, $E = -0.4$ V *vs* E^0) and oxidation (panel b, $E = 0.4$ V *vs* E^0). The quasi-rectangle distribution on the left side of each panel represent the electrode DOS; the Gaussian distributions on the right side of each panel represent the redox DOS. The shaded areas indicate the occupied states.

potentials far removed from E^0, the BV model would be problematic in predicting the voltammetric responses. There are a few recent theoretical studies demonstrating the deficiency of the BV model at electrodes having electroactive radii of nanometer scales, at which the MT layers are reduced to nanometer scales, and therefore high MT rates of electroactive species are achieved.[18−20] Similar to electrode of nanometer sizes, nanometer-wide thin-layer cells also offer extremely high MT rates by confining the MT processes in nanometer domains.

The limitation of the linear-free-energy approximation can be overcome by adopting more realistic quadratic free energy relations, as done in the Marcus−Hush (MH) ET theory, which was originally developed by Marcus for homogeneous ET kinetics and modified for treating heterogeneous ET kinetics mainly by Marcus and Hush.[17,21−23] The MH treatment provides more physical insight into outer-sphere ET kinetics by relating the activation of ET processes with the reorganization of redox species together with their solvent shells. In both of the BV and classic MH models, the effect of the electrode potential (E) on ET rates is treated by modifying the free energy of reaction with the product of E and the Faraday constant (F). Doing this implies that only the electronic states at the Fermi level of electrode are involved in an ET reaction; in the meantime the redox agents have to reorganize themselves to an activation configuration that possesses a frontier electronic state (HOMO or LUMO) aligned with the Fermi level of electrode. It has been long recognized that heterogeneous ET involves electron-tunneling over a range of energy levels between the electrode continuum and the frontier electronic states of the redox agents, which are broadened to a Gaussian type of distribution due to structure reorganization (Figure 1).[17,24−26] The classic MH and BV formalisms have simplified the multilevel, multistate heterogeneous ET into an equivalent narrow one-level, two-state ET around the Fermi level. Such simplification would be reasonable if the electron accepting (unoccupied) and giving (occupied) states vary little in density along the energy levels in the overlapped region, which is obviously not true when considering the Gaussian distribution of density of states (DOS) of the redox agents. Only as E falls in the narrow region near E^0 in which the redox DOS is very low and relatively flat, does the overall overlapped areas between electrode and the redox DOS remain nearly constant along the energy levels. To this end, voltammetric treatments of redox cycling in the thin-layer cells of nanometer width have to explicitly deal with the DOS overlap between electrodes and redox agents due to the extension of the ET kinetics governed voltammetric behavior to higher overpotentials.

In addition to the possible failure of the linear-free-energy and two-state approximations in ET kinetics, confining electrode reactions in nanometer-wide domains also challenges the conventional voltammetric treatments by raising significant electric-double-layer (EDL) effects on ET kinetics and MT dynamics.[27−31] In this case, the classic diffusion and/or diffusion/electromigration treatments of MT based on the assumption of electroneutrality in the MT layers may be inappropriate. Similarly, the diffuse EDL would become highly dynamic due to the extremely high MT rates of redox ions, so that the Frumkin correction that is based on equilibrium EDL theory may fail to account for the diffuse EDL effects on heterogeneous ET kinetics.[30,31]

In this paper, we use finite-element simulations to investigate the steady-state voltammetric behaviors of fast outer-sphere redox couples (O^z/R^{z-1}) in thin-layer cells defined by two parallel electrodes which are separated by nanometer-wide electrolyte solution (Figure 2). To gain insights into the applicability of the classic BV and MH theories, the voltammetric responses predicted by these models are compared with that given by the more realistic Marcus−Hush−Chidsey (MHC) model developed by Chidsey.[24] In the MHC model, the earlier theoretical treatments

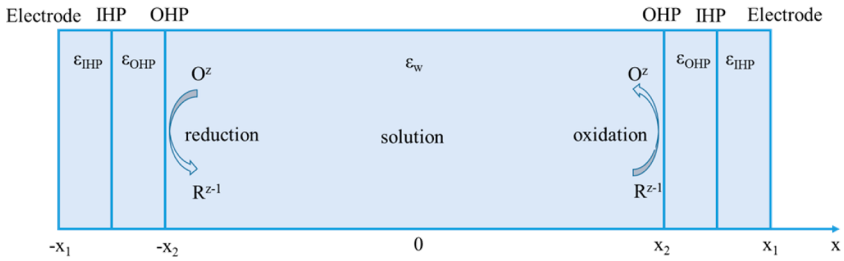

Figure 2. Schematic diagram of the cross section of the thin-layer cell bounded by two electrodes of infinite sizes between which the redox couple of O^z/R^{z-1} are repeatedly oxidized and reduced. Gap distance $L = 2x_1$; Outer Helmholtz planes (OHPs) at $\pm x_2$ are assumed to correspond to the position of the closest approach (PCA) of solvated species to the electrodes and, thus, are set as the reaction planes. The compact EDL at each electrode is divided into two parts by the inner Helmholtz planes (IHP). The thickness of the compact EDLs ($\mu = x_1 - x_2$) is estimated to be *ca.* 0.6 nm.[30−32] The ε_{OHP}, ε_{IHP} and ε_w define the dielectric constant of water in different regions: inside the IHP, between IHPs and OHPs, and outside the OHPs. See text and Models and Simulations for more details.

by Levich[25] and Gerischer[26] that deal with the multilevel, multistate nature of the heterogeneous ET processes on the basis of DOS overlap between electrode and redox molecules, and the classic MH formalism that accounts for the ET kinetics at individual electronic energy levels using a quadratic free energy relation, are integrated to produce rate constant expressions.[18,19] The comparison is presented by systematically varying the gap width between two electrodes and the kinetics parameters of the ET reactions such as rate constants and reorganization energies. The EDL effects on the ET and MT rates are investigated as functions of electrode gap width and redox charges, by combining the MHC model and the Poisson−Nernst−Planck (PNP) theory. The simulations lead to the conclusion that the conventional voltammetric theory based on the BV kinetic model combined with the diffusion transport equations may incorrectly predict voltammetric responses for redox agents with relatively slow ET kinetics and low reorganization energies in very narrow cells. However, one may still use the conventional voltammetric theory to extract the fast ET kinetics and to perform voltammetric detection using nanometer-wide thin-layer cells of properly chosen gap width. We also show that the quadratic MH rate constant expressions can be an alternative to the mathematically complex integration in the MHC formalism for treating the voltammetric responses of thin layer cells of larger than 20 nm gap width, except for redox couples which simultaneously have sluggish ET kinetics and small reorganization energies.

RESULTS AND DISCUSSION

Applicability of the Classic BV and MH Theories in Predicting the Voltammetric Responses. As discussed above, the classic BV and MH theories become increasingly inappropriate when E is far from E^0. It is known that the ET kinetics-governed voltammetric response would extend to potentials increasingly removed from E^0 with increasing irreversibility of electrode reaction.[17] The latter can be described by the dimensionless ratio of the ET rate constant at the formal potential of the redox couple (k^0) and the MT coefficient of the redox couple (m), $\gamma = k^0/m$. In thin-layer cells considered here, $m = 2D/L$, in which D is the diffusion coefficient of the redox couple, and L is the gap distance between the two electrodes in the cell. In addition, the deficiency of the two-state ET assumption in the BV and MH theories would also become pronounced for redox couples with decreased reorganization energy (λ).[18−20] As manifested in Figure 1, a small λ value corresponds to the redox DOS distribution mainly near energy levels close to E^0. Accordingly, the overlapped areas between electrode and redox DOS significantly vary with energy levels even at low overpotentials ($|E - E^0|$). For a redox couple with large λ value, the redox DOS in a wide range of energy levels around E^0 is nearly flat, which makes the overlapped DOS areas between electrode and redox agents remain approximately invariant in a wide range of electrode potentials from E^0. In the following, we investigate the deviation of the BV and MH predictions from that of the MHC formalism by varying L, λ and k^0.

In order to clearly show the effect of using different ET kinetics theories, the simulations on the voltammetric responses of thin-layer cells in this subsection are performed by ignoring the possible EDL effects. To do so, Fick's diffusion equations are used to treat the mass transport and concentration distribution of redox agents in the domain between two outer Helmholtz planes (OHPs) (Figure 2, also see Models and Simulations for the main and boundary equations and the simulation parameters), in combination with the reaction rate equations in which the rate constant expressions given in the BV, MH or MHC theories are used (see Models and Simulations for details). In these theories, the ET rate constants vary with E in different manners. The BV theory predicts an exponential increase of rate constants as the overpotential ($|E - E^0|$) increases, while the rate constants in the MH theory exhibit a maximum at moderately high overpotentials, after which the rate constants decrease with removing E from E^0, forming the so-called Marcus inversion region of ET kinetics.[17] According to the MHC model, however,

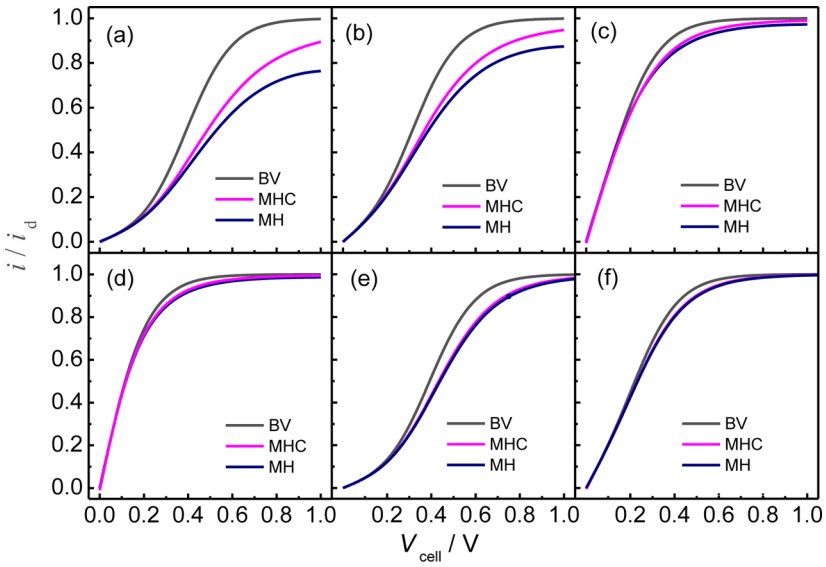

Figure 3. Normalized steady-state polarization curves calculated by using different ET kinetic models and pure diffusion MT equations for one-electron ET reactions for redox couples having a k^0 value of 1 cm/s and λ values of (a−d) 50 kJ/mol λ and (e,f) 100 kJ/mol, respectively. The values of L are, respectively, (a) 10 nm, (b) 20 nm, (c) 100 nm, (d) 200 nm, (e) 10 nm, and (f) 50 nm.

the rate constants reach a limiting value at some large $|E - E^0|$, at which the overlapped area between electrode and redox DOS approximately reaches a maximum and changes little upon further increasing the $|E - E^0|$ value.[18−20]

We first consider the one-electron ET reaction for redox couples having a typically high k^0 value of 1 cm/s and different λ values in thin-layer cells of different L. The steady-state current responses upon varying the cell voltage (V_{cell}), predicted by different ET kinetic models, are shown in Figure 3. Only the anodic polarization curves are given; because of the cell symmetry, the cathodic curves have identical shapes. In addition, the currents in the polarization curves have been normalized by the limiting diffusion currents (i_d) calculated according to, $i_d = FD(c_O^* + c_O^*)/(L - 2\mu)$, where c_O^* and c_R^* are the initial concentrations of the redox couple in the cells, and $\mu = x_1 - x_2$ is the thickness of the compact EDL (Figure 2). One can observe from Figure 3 that the polarization curves become drawn out with decreasing gap distance, indicating increasing irreversibility of electrode process. As compared to the prediction of the MHC model, the BV and MH theory overestimates and underestimates, respectively, the voltammetric currents for small gap distances. For a redox couple with λ = 50 kJ/mol, the limiting diffusion current is no longer accessible within the MHC and MH models when the gap distances are less than 100 nm. This is due to values of i_d in the narrow thin-layer cell being considerably larger than the limiting kinetic current under the MHC formalism and the maximum current predicted by the MH model. For a given L, the MH theory stays valid in a wider potential range than the BV theory. When L is *ca.* 50 nm or larger, the MH and MHC formalisms are found to give very similar prediction at potentials prior to the occurrence of Marcus inversion. As L is larger than 200 nm, the three models are nearly undistinguished in predicting the voltammetric responses. For redox couple with λ = 100 kJ/mol, the MH model gives nearly identical prediction to that of the MHC model in thin-layer cells with gap distance as narrow as 10 nm (Figure 3e), and the limiting diffusion current could be accessible under all the three ET models in this case. Upon increasing the gap distance to 50 nm (Figure 3f), the voltammetric responses predicted by the three models tend to converge.

Figure 4 compares the polarization curves for redox couples with a relatively small k^0 value (0.1 cm/s). Because of the increased irreversibility of electrode reaction, the deviation of BV and MH prediction is more pronounced than that seen in Figure 3, especially for redox couples with λ = 50 kJ/mol (panels a, c, and e). For λ = 100 kJ/mol, however, the MH model still predicts very similar voltammetric responses to the MHC model for various L (panels b, d, and f). As for the BV model, the predicted voltammetric responses deviate significantly from that of the MH and MHC model even when gap distance are as large as 100 nm. We found that the polarization curves calculated with the BV model coincide with that given by the MH and MHC formalisms as L increases to *ca.* 400 nm for ET reaction of such small k^0. Considering that small k^0 values usually are associated with large λ, the cases shown in Figure 4a, c and e should be rarely seen. To this end, we may conclude from the results shown in Figures 3 and 4 that the MH formalism can be a reasonable alternative to the complex MHC model in describing the voltammetric responses of thin-layer cells, except for the ET reaction of very small λ at

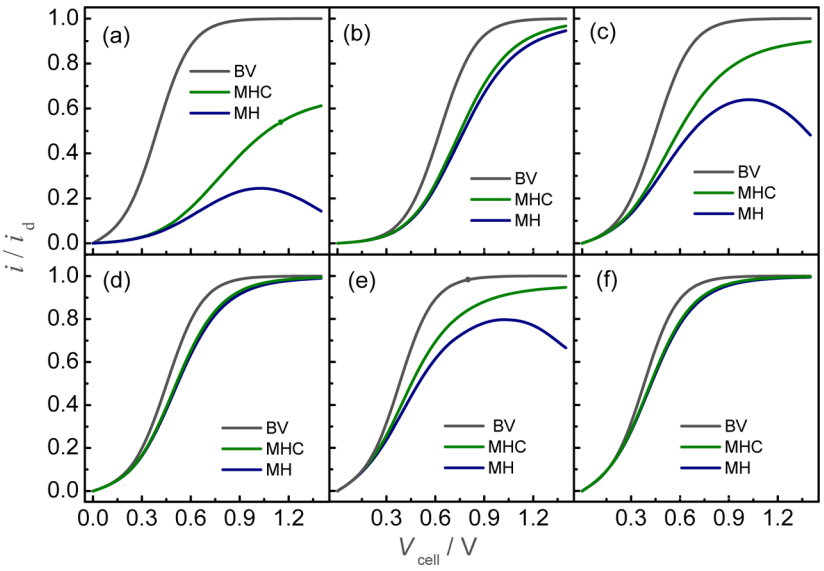

Figure 4. Normalized steady-state polarization curves calculated using different ET kinetic models under pure diffusion conditions for one-electron ET reactions for redox couples with a relatively small k^0 value (0.1 cm/s) and different λ values in thin-layer cells of different gap distances: (a) L = 10 nm, λ = 50 kJ/mol; (b) L = 10 nm, λ = 100 kJ/mol; (c) L = 50 nm, λ = 50 kJ/mol; (d) L = 50 nm, λ = 100 kJ/mol; (e) L = 100 nm, λ = 50 kJ/mol; (f) L = 100 nm, λ = 100 kJ/mol.

electrodes separated by very narrow distances, *e.g.*, $\lambda < 50$ kJ/mol and $L < 20$ nm.

EDL Effects on the Voltammetric Responses. Given that the BV and MH models have been shown above to yield inaccurate predictions of the voltammetric responses for redox reactions with small λ and k^0 in nanometer-wide thin-layer cells, we investigated the EDL effects in thin-layer cells under the MHC scheme, by solving the PNP equations in combination with reaction rate equations in which the MHC rate constant expressions are used. The PNP equations deal with the coupling between electric potential and concentration distributions in the cells. The Poisson equation is solved in the entire spatial region between two electrodes ($-x_1 < x < x_1$), while the Nernst−Planck equation is solved in the region between two OHPs (Figure 2, also see Models and Simulations for the main and boundary equations and the simulation parameters). When solving the Poisson equation, a 3-state dielectric model for solvent molecules is employed to define the dielectric constant of water (ε) of the different regions in thin-layer cells, namely, $\varepsilon = 6$ inside the IHPs, $\varepsilon = 40$ between IHPs and OHPs, and $\varepsilon = 78$ outside OHPs (Figure 2).[30−33] It has been shown that this simple dielectric model reasonably describes the coupling between the electric potential distribution and the solvent dielectric distribution at electrode/electrolyte interface; ignoring the interaction between the electric field and the solvent dielectric field would lead to unrealistic prediction of EDL effects on voltammetric responses.[30,31] In the simulations, we introduce a 1:1 electrolyte with a concentration of 500 mmol/L, which is in excess of the 1 mmol/L redox species. In this case, the conventional Frumkin diffuse EDL effect would be negligible. Therefore, the observed EDL effects in this study should be mainly a result of the confinement of electrode reaction in nanometer domains.

The EDL effect on the voltammetric responses of thin-layer cells depend on the charges of the redox species and the reversibility of ET processes. The latter is related to the gap distances and the rate constant of the ET reaction. We first investigate a relatively facile one-electron ET reactions (k^0 = 1 cm/s) of differently charged redox couples in a 10 nm wide cell. Figure 5a displays the calculated polarization curves for redox couples of O^z/R^{z-1} with $z \geq 0$. The charge-independent polarization curve calculated without considering the EDL effect is also given (black dotted line) for comparison. One can see that the voltammetric currents for $z > +1$ are inhibited when the EDL effect is included in the calculation. The inhibition magnitude increases with increasing z. It is known that the EDL effect inhibits the reduction of negatively charge species or the oxidation of positively charged species, and enhances the reduction of positively charged species or the oxidation of negatively charged species. For a redox couple O^z/R^{z-1} with $z > +1$, one would expect opposite EDL effects at the two thin-layer cell electrodes. Note that the electrode where the ET rate is slower inhibits the overall cell current since the currents at the anode and cathode are equal in magnitude. For redox couples of O^z/R^{z-1} with $z < 0$, the situation would be the same as that for $O^{|z|+1}/R^{|z|}$, because in these cases the voltammetric currents are limited respectively by the reduction of O^z and the oxidation of $R^{|z|}$, which should undergo the same inhibition magnitude by the EDL effect due to the same redox charges.

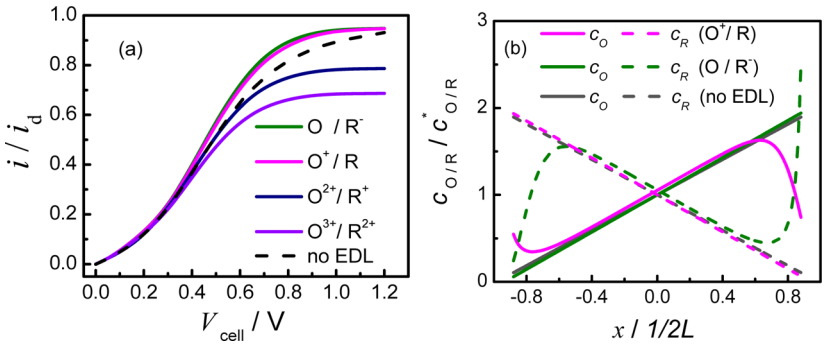

Figure 5. (a) Calculated steady-state polarization curves for one-electron ET reactions, $O^z + e^- \leftrightarrow R^{z-1}$ with different z, in the presence of a 1:1 supporting electrolyte (M^+N^-) in a 10 nm thin-layer cell using the MHC ET kinetic model with and without consideration of the EDL effect. (b) Concentration profiles of the redox species for z = 0 and +1 at V_{cell} of 1 V. Other parameters: k^0, 1 cm/s; λ, 50 kJ/mol.

In the cases when z = 0 and z = +1, the overall currents should be limited, respectively, by the reduction of the neutral O or the oxidation of the neutral R. Therefore, the polarization curves are nearly identical to each other. Since the ET rates of neutral species are negligibly impacted by the EDL, one may expect that the voltammetric currents in the two cases would be identical to that in the absence of EDL effect. As shown in Figure 5a, this seems to be true only at considerably large cell voltages where the limiting currents are reached; otherwise the calculated currents are generally larger than that in the absence of EDL effect. The net current at an electrode should be a result of the oxidation and reduction. Although the reduction rate of neutral O at the left electrode is not affected by the EDL in the case that $z = 0$, the rate of the oxidation of R^- could be affected at this electrode. As shown in Figure 5b, the EDL effect results in significantly depletion of R^- (green dash line) as compared with that in the absence of EDL effect at the left OHP, which would lead to decrease in the oxidation rate of R^-. Consequently, the net current at the left electrode is larger than that in the absence of the EDL effect. At very large cell voltage, the overpotential for the oxidation of R^- at the left electrode would be very low, so that the oxidation direction contributes little to the net current. A similar explanation can be made for $z = +1$ according to the concentration profiles shown in Figure 5b.

In Figure 6, the steady-state polarization curves for the one-electron ET reaction of $O^{3+} + e^- \leftrightarrow R^{2+}$ with k^0 equal to 1.0 and 0.1 cm/s in 50 and 100 nm wide thin-layer cells calculated by using the MHC ET kinetic model, with and without consideration of EDL effect, are compared. As seen in Figure 6a and 6b, the EDL effect becomes much less pronounced in thin-layer cells of 50 and 100 nm width for the relatively facile ET reaction (k^0 = 1.0 cm/s) in comparison with that in the 10 nm wide cell shown in Figure 5. Even for this highly charged redox couple, the EDL effect only results in less than 10% inhibition of limiting current, while the kinetics-controlled currents are nearly unaffected. For

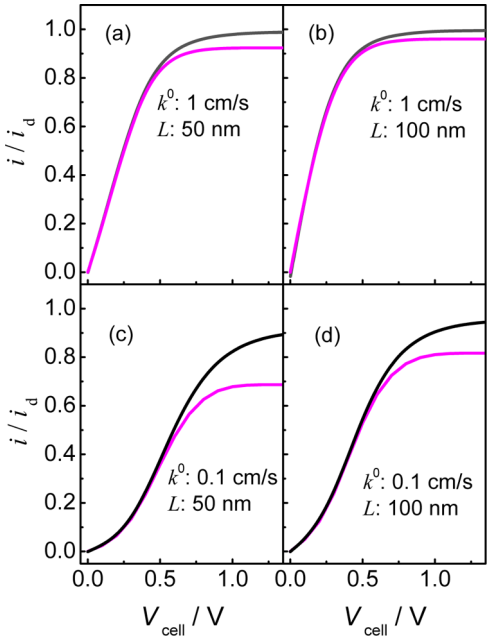

Figure 6. Calculated steady-state polarization curves for the one-electron ET reaction, $O^{3+} + e^- \leftrightarrow R^{2+}$, with k^0 equal to (a,b) 1.0 cm/s and (c,d) 0.1 cm/s, in the presence of a 1:1 supporting electrolyte (M^+N^-) in (a,c) 50 nm and (b,d) 100 nm wide thin-layer cells by using the MHC ET kinetic model with (magenta) and without (black) consideration of EDL effect. The other parameters are the same as that for Figure 5a.

the redox couple having the same charges but a relatively slow ET kinetic rate constant of 0.1 cm/s, the EDL effect results in *ca.* 20% inhibition of the limiting current in these wider cells (Figure 6c and 6d). One should expect more pronounced inhibition of voltammetric responses by the EDL effect upon further decreasing the k^0 value.

On the Voltammetric Analysis Using Nanometer-Wide Thin-Layer Cells. The above simulations have indicated that the common voltammetric treatment, based on the BV ET kinetics theory without considering EDL effects, could become inappropriate for electrode reactions in nanometer wide thin-layer cells. However, considering the mathematic straightforwardness, the conventional

TABLE 1. Ratios of the Limiting Currents Predicted by the MHC ET Kinetic Model When Considering the EDL Effects (i_L) over the Conventional Diffusion Limited Current (i_d) for One Electron ET Reactions, $O^z + e^- \leftrightarrow R^{z-1}$, with Different z and k^{0a}

	i_L/i_d					
	$z = +3$		$z = +2$		$z = +1$	
L	$k^0 = 1$	$k^0 = 0.1$	$k^0 = 1$	$k^0 = 0.1$	$k^0 = 1$	$k^0 = 0.1$
(nm)	cm/s	cm/s	cm/s	cm/s	cm/s	cm/s
10	0.69	0.27	0.79	0.39	0.95	0.63
50	0.92	0.69	0.95	0.78	0.99	0.90
100	0.96	0.82	0.98	0.88	1.00	0.95

[a] Other parameters are the same as that for Figure 5.

treatment may remain in use by researchers performing voltammetric analysis. An important question is in what conditions and to what extent this treatment can be used. This should be considered in two major applications of thin-layer cells, namely, voltammetric detection and ET kinetics determination.

Limiting Current Based Voltammetric Detection. In voltammetric sensing application, the limiting currents are mostly used since they are related to the concentration of electroactive species. In Table 1, we list the ratios of the limiting currents (i_L), predicted by the MHC ET kinetic model when including the EDL effect, to the conventional diffusion-limited currents (i_d) predicted by the BV model without considering the EDL effects, for one-electron ET reactions ($O^z + e^- \leftrightarrow R^{z-1}$) with different k^0 and z in thin-layer cells of different width. One finds that in all the cases the i_L is smaller than i_d, which is a consequence of the intrinsic MHC ET kinetic and EDL effects. In the case that the ET kinetics is relatively facile (k^0 = 1 cm/s), the depression is *ca.* 30% or less in magnitude, regardless of the charges of the redox species and the cell width. For the relatively slow ET reactions (k^0 = 0.1 cm/s) of highly charged redox couple ($z = +3$) in 10 nm wide cell, the current is depressed up to *ca.* 70%. In thin-layer cells of 50 nm and larger width, however, the current depression is within 30% for reactions with k^0 = 0.1 cm/s.

Normally, a deviation of several tens of percent from the real values would represent a significant detection error. For voltammetric sensing which requires ultrahigh sensitivity, however, this error may be within an acceptable limit since the concentrations of the detected electroactive species should be extremely low. Thus, the conventional voltammetric theory may be used to treat the sensing data obtained by using thin-layer cells wider than 50 nm, unless the electroactive species has an ET rate constant less than 0.1 cm/s. For electroactive species with very sluggish ET kinetics, it would be unwise to perform voltammetric detection using the nanometer wide thin-layer cells, since the effect of the intrinsic MHC ET kinetics and EDL not only complicate the data analysis, but also negate the amplification effect of the nanometer wide cells.

Fast ET Kinetics Analysis. For ET kinetics analysis based on the steady-state voltammetric responses, it is essential that the associated electrode process is at least partially governed by the ET kinetics; *i.e.*, the reaction is quasi-reversible. This can be represented by a significant shift of the half-wave potential ($E_{1/2}$), which refers to the potential where the current density reaches half of the limiting value, as a function of γ (= $k^0L/2D$). When both O and R are initially present, the $E_{1/2}$ *vs* γ relation can be expressed by eq 1, according to the steady-state voltammetric equation based on the BV kinetic model and the diffusion mass transport equations.[17]

$$E_{1/2} = E^0 \pm \frac{RT}{\alpha F} \ln\left(\frac{1+\sqrt{1+12\gamma^2}}{2\gamma}\right) \qquad (1)$$

In eq 1, the sign ($\pm$) is positive for the anodic polarization curves and negative for the cathodic ones. Figure 7a gives the plot of the anodic $E_{1/2}$ as a function of γ predicted by eq 1, which indicates a significant variation in $E_{1/2}$ as γ decreases to values below 2.5. For moderately fast ET reactions; *e.g.*, those having a k^0 of *ca.* 1 cm/s, gap distances should be 500 nm or larger to achieve this γ value. As shown from the above simulation results, the use of BV model and ignoring the EDL effect on ET kinetics would cause little deviation of steady-state voltammetric responses from that obtained by using the more realistic MHC formalism when considering the EDL effect in the cases that k^0 = 1 cm/s and L > 100 nm. To this end, the conventional BV-based voltammetric analysis using thin-layer cells of 100−500 nm widths should be able to provide reliable ET kinetics of k^0 around 1 cm/s.

To investigate ET kinetics faster than 1 cm/s, thin-layer cells of smaller gap distances are required. For k^0 = 10 cm/s, for example, cell widths should be around 50 nm or smaller to achieve a γ value of 2.5. Figure 7b displays the steady-state polarization curves for such fast one-electron ET reactions of differently charged redox couples in a 20 nm wide cell. Since both the MHC kinetics and the EDL effect would result in depressed current in nanometer wide dells in comparison with that given by the conventional voltammetric theory, one would expect that the apparent rate constant (k^{0a}) estimated from a measured polarization curve using the conventional theory would be lower than the real k^0. However, it can be seen from Figure 7b that the current depression occurs mainly in the limiting current region. The decrease in the limiting current would yield an $E_{1/2}$ value closer to E^0 (V_{cell} = 0 for thin-layer cells) than that predicted by the conventional voltammetric theory. This can be more clearly seen by the enlarged portion of the current−potential curves near $E_{1/2}$ as shown in Figure 7c, in which the currents are normalized by i_L instead of i_d.

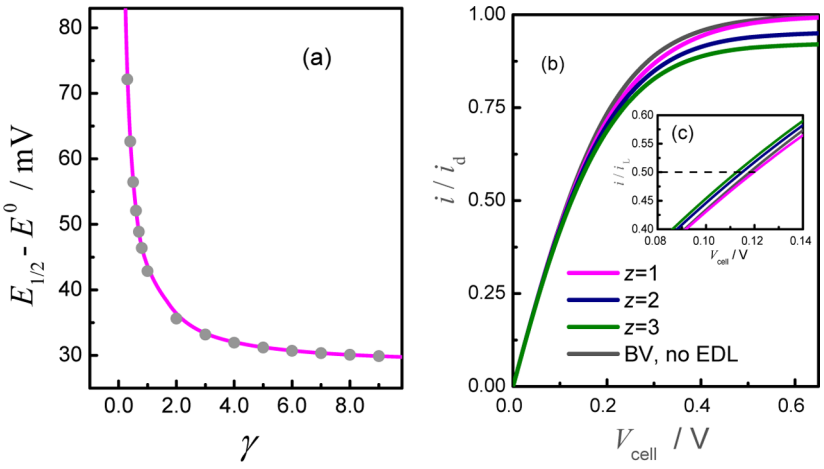

Figure 7. (a) $E_{1/2}$ *vs* γ relation predicted by eq 1. (b) Steady-state polarization curves for one-electron ET reactions, $O^z + e^- \leftrightarrow R^{z-1}$, with k^0=10 cm/s, in a 20 nm wide thin-layer cell, calculated using the MHC ET kinetic model with consideration of EDL effect, and by using the BV model without consideration of EDL effect (black). (c) Polarization curves in (b) given with currents being normalized by i_L and the parts around $E_{1/2}$ being enlarged. Other parameters are the same as that for Figure 5a.

TABLE 2. $E_{1/2}$ Values on Polarization Curves for ET Reaction of 10 cm/s k^0 and Differently Charged Redox Couples and the Resulted Apparent Rate Constants (k^{0a})

	$z = +3$		$z = +2$		$z = +1$		
L (nm)	$E_{1/2}$ (mV)	k^{0a} (cm/s)	$E_{1/2}$ (mV)	k^{0a} (cm/s)	$E_{1/2}$ (mV)	k^{0a} (cm/s)	$E_{1/2}{}^a$ (mV)
10	154.8	11.8	160.9	10.92	173.7	9.33	168
20	110.6	11.1	112.6	10.69	117.6	9.73	116.1
50	78	11.2	78.8	10.80	80.3	10.08	80.5

[a] $E_{1/2}$ values predicted by voltammetric theory based on the BV kinetic model and the diffusion transport equations

When these $E_{1/2}$ values are used to calculate rate constants according to eq 1, apparent values higher than the actual k^0 will be obtained. As shown in Table 2, however, the deviation of k^{0a} from k^0 are generally within 20%. This should be in an acceptable range of deviation error in usual most electrochemical analyses.

A Brief Discussion on the Effect of Nonidealized Electrode Geometries. It should be emphasized that the results and discussion presented above are based on models in which the two electrodes in thin-layer cells have infinite sizes and ideally smooth surfaces. Practically, the electrodes in various thin-layer cell devices may not have such idealized geometries. The assumption of infinite electrode size has allowed us to ignore the edge and misalignment effects of the electrodes, so that the concentration and potential profiles in the thin-layer cells can be modeled with a one-dimensional (1-D) geometry as that shown in Figure 2. At the edge of a planar electrode, the concentration and potential fields will be nonuniform along the electrode surface and no longer 1-D in nature. The electrode edge effect on the mass transport dynamics has been an important issue in the voltammetric treatments of micrometer-sized planar electrodes.[17,34] In general, the edge effects at planar electrodes in bulk solution would enhance the current density due to the multidimensional converging mass transport of electroactive agents. In thin-layer cells, however, the open geometry at the electrode edge would weaken the voltammetric amplification due to redox cycling of electroactive agents becoming less efficient. The misalignment between two electrodes in the thin-layer cells would enhance the electrode edge effect. The overall effects of the finite size and misalignment of the electrodes in a thin-layer cell should depend on the electrode dimension, the gap width and the degree of the misalignment between two electrodes. The influence of the edge and misalignment effects would become more pronounced in cells with smaller gap width or electrodes of smaller sizes. In typical thin-layer cell devices with nanometer gap width, the electrode dimensions should be much larger than the gap width. In this case, the nonuniform distributions of concentrations and potential at electrode edges should have negligible influence on the overall voltammetric responses. In addition, modern fabrication techniques allow relatively precise control of electrode geometry and location, which should avoid the large degree of electrode misalignment. Therefore, the assumptions on the infinite size and alignment of electrodes in the present study should not affect the applications of the obtained results and conclusions in nanometer-wide thin-layer cell experiments.

The surface roughness of electrode is a common feature in electrochemical experiments. The direct effect of surface roughness is an increase in the real active area of electrode, which is equivalent to an apparent increase in the rate constant of the ET reaction, and, therefore, an increase in the reversibility of electrode processes. As shown by the results presented above, the increase in the reversibility of electrode processes would weaken both the intrinsic MHC kinetic

and the EDL effects on the voltammetric responses in thin-layer cells. This not only makes the conventional voltammetric treatments applicable to narrower cells, but also results in increased voltammetric currents. To a first approximation, experimental results obtained in a thin-layer cell consisting of electrodes with a roughness factor of R may correspond to the simulation results for reactions with k^0/R presented above. In the case that the electrodes are very rough and even porous, the mathematic and geometric models in the present studies should be modified to reliably simulate the corresponding voltammetric responses. Nowadays, the electrodes in nanometer-wide thin-layer cells are mostly thin metal films fabricated by vapor deposition or sputtering, which should result in relatively smooth electrodes.[7,8]

CONCLUSION

The voltammetric behaviors associated with redox cycling of electroactive molecules in thin-layer cells between two electrodes separated by nanometer width have been systematically simulated by using different ET kinetic models and by considering the possible EDL effects. The results indicate that the conventional voltammetric theory based on the BV kinetic model and the diffusion transport equations may predict voltammetric responses that deviate from those predicted by the more realistic MHC ET kinetic model combined with Poisson-Nernst−Planck equations that account for the effects of EDL. The magnitudes of the deviation depend on the gap widths (L) and the parameters of the ET reactions such as k^0, λ and charges of the redox couple (z). In general, more pronounced deviation occurs as L, k^0 and λ are smaller, and as z is larger.

For one-electron reactions with a typical k^0 of 1 cm/s and λ of 100 kJ/mol, the BV model may become inappropriate as L is reduced below 50 nm, whereas this limitation occurs for $L < 400$ nm for reactions with 0.1 cm/s k^0. For fast ET reactions (*e.g*, $k^0 = 10$ cm/s), the BV model can be approximately applied in thin-layer cells as small as 20 nm in width. In most cases, the classic MH model gives very similar prediction of voltammetric responses to that predicted by the MHC model, except for ET reactions with very small λ (*e.g.*, < 50 kJ/mol) in very narrow cells ($L < 20$ nm). Therefore, the mathematically complex integration in the MHC formalism may be replaced by the quadratic MH equation for ET rate constants in treating the voltammetric responses of thin layer cells larger than 10 nm gap distances.

The EDL structures may visibly affect the voltammetric responses of thin-layer cells of gap width less than 50 nm in widths for ET reactions with typical k^0 of 1 cm/s. For reactions with smaller k^0 values, the EDL effect would be apparent at larger gap width. For redox couple of the same sign, *i.e.*, for O^z/R^{z-1} of $z > +1$ or < 0, the EDL effect inhibits the currents at all potentials. In the cases that $z = +1$ or 0, the limiting currents are negligibly affected by the EDL structures since they are governed mainly by the reduction or oxidation of the noncharged species; however, the currents in the kinetics-controlled region are slightly enhanced because the inhibition of the backward reaction by the EDL.

By properly choosing gap widths such that the EDL effect and the ET kinetic models do not make substantial difference to the voltammetric responses, one may still use the conventional voltammetric theory based on the BV kinetic model and diffusion transport equations to extract fast ET kinetics from the steady-state voltammetric responses of thin-layer cells. For example, the classical treatment would apply to 100−500 nm wide cells for k^0 of ~1 cm/s, and to 20−50 nm wide cells for ET kinetics for k^0 of ~10 cm/s. As for the voltammetric detection, the conventional voltammetric theory may be used to analyze data obtained by using thin-layer cells wider than 50 nm, unless the ET rate constant is less than 0.1 cm/s. For electroactive species with very sluggish ET kinetics, it would be unwise to perform voltammetric detection using the nanometer-wide thin-layer cells, since the effect of the intrinsic MHC ET kinetics and EDL not only complicate the data analysis, but also negate the amplification effect of the nanometer wide cells.

MODELS AND SIMULATIONS

The simulations were performed using the finite element method in the COMSOL Multiphysics package (http://www.comsol.com). It is assumed for simplicity that all species have the same diffusion coefficients ($D = 2 \times 10^{-5}$ cm^2/s). The effects of the finite sizes of ions and the solvent noncontinuum are ignored (except for the assumption that the closest approach of the redox ions to the electrodes is the OHP). It is also assumed that none of the ions in the solution specifically adsorbs on the electrode surface, *i.e.*, no charge resides in the compact part of the double layer. The electrode potentials are quoted with respect of the potential of the zero charge (PZC).

When the effect of the EDL structures is considered, the steady-state electrostatic potential and concentration distributions in the gap regions are modeled with the Poisson−Nernst−Planck (PNP) equations, with the Poisson equation (eq 2) formulating the local electric potential (ϕ) in a dielectric medium, and the Nernst−Planck equation (eq 3) describing the transport of solution species. The domain for solving the Poisson equation is the entire spatial region ($-x_1 < x < x_1$) in the cell, while the Nernst−Planck equation is solved in the region between two OHPs.

$$\nabla^2\phi = \frac{\partial^2\phi}{\partial x^2} = -\frac{\rho}{\varepsilon_0\varepsilon} \tag{2}$$

$$D\frac{\partial^2 c_i}{\partial x^2} + \frac{\partial}{\partial x}\left(Dc_i\frac{F}{RT}\nabla\phi\right) = 0 \tag{3}$$

In eq 2, ε_0 and ε refer to the permittivity of the vacuum and the local dielectric constants of water respectively, ρ is the local

charge density, which is zero in the compact EDLs ($-x_1 < x < -x_2$ and $x_2 < x < x_1$) and equals to $F\Sigma z_i c_i$ (z_i and c_i refer to the charge and the local concentration of species i respectively) outside of the OHPs; F, R, T have their usual meanings. To solve the PNP equations, the following boundary conditions are used.

At the right electrode surface ($x = x_1$),

$$\phi = E_{ox} \tag{4}$$

At the right OHP ($x = x_2$),

$$\frac{\partial c_i}{\partial x} = \frac{m_i j_{ox}}{FD} \tag{5}$$

in which j_{ox} is the current density at the right electrode surface, m_i is an integer constant and takes values of 1, −1, and 0 for species O^z, R^{z-1}, and the inert electrolyte species (M^+ and N^-). And

$$j_{ox} = -F(k_c c_O - k_a c_R) \tag{6}$$

where k_c and k_a are the rate constants for the reduction and oxidation direction which are expressed differently according to the ET kinetic models used (eq 13−15). At the left electrode surface ($x = -x_1$),

$$\phi = E_{red} \tag{7}$$

$$E_{red} = E_{ox} - V_{cell} \tag{8}$$

At the left OHP ($x = -x_2$),

$$\frac{\partial c_i}{\partial x} = -\frac{m_i j_{red}}{FD} \tag{9}$$

in which j_{red} is the current density at the left electrode surface, and

$$j_{red} = F(k_c c_O - k_a c_R) \tag{10}$$

$$j_{red} = j_{ox} \tag{11}$$

In the case when EDL effects are not considered, the PNP equations are replaced by the steady-state Fick's diffuse equations, *i.e.*,

$$D\frac{\partial^2 c_i}{\partial x^2} = 0 \tag{12}$$

To solve eq 12, the boundary conditions of eq 4 and 7 are not required since the electrostatic potential is not included in eq 12. The expressions of k_a and k_c in different ET kinetic models are as follows.

$$k_{a/c}^{BV} = k^0 \exp(\pm F(E - \phi_{OHP} - E^0)/2RT) \tag{13}$$

$$k_{a/c}^{MH} = k_{a/c}^{BV} \exp(-F^2(E - \phi_{OHP} - E^0)^2/4\lambda RT) \tag{14}$$

$$k_{a/c}^{MHC} = k_{a/c}^{BV} \frac{\int_{-\infty}^{+\infty} \frac{\exp(-F^2(\varepsilon - E^0)^2/4\lambda RT)}{2\cosh(F(\varepsilon - E)/2RT)} d\varepsilon}{\int_{-\infty}^{+\infty} \frac{\exp(-F^2(\varepsilon - E)^2/4\lambda RT)}{2\cosh(F(\varepsilon - E)/2RT)} d\varepsilon} \tag{15}$$

In eqs 13−15, $E = E_{red}$ or E_{ox} for the reduction (c) or the oxidation (a), respectively, ϕ_{OHP} is the electric potentials at the corresponding OHPs, E^0 is the formal electrode potential which is considered equal to the potential of PZC in the present calculations, k^0 is the formal ET rate constant at E^0, and λ is the reorganization energy of the redox couple. We have assumed the electron transfer coefficient $\alpha = 0.5$ in the BV model by using eq 13. In the case when the EDL effects are not considered, E-ϕ_{OHP} in the above equations is replaced by E.

To solve the governing equations in a thin-layer cell in the COMSOL Multiphysics package, the gap region between two electrodes is divided into 1-D mesh elements of different length. In the domains within the OHPs and *ca.* 1 nm outside the OHPs, the finest mesh elements of 0.005 nm length are used. The mesh length is then gradually increased with distance from the OHPs. The total number of the mesh elements is about 1200 for 100 nm gap and 800 for 10 nm gap. The largest mesh length is 0.05 nm for 10 nm gap and 0.2 nm for 100 nm gap. The use of such nonuniform mesh elements can accurately capture the rapid variation of potential and concentrations in the spatial region near the electrode surfaces without significantly increasing the computation time. Two weak constraints were used to define the boundary equations of eq 8 and eq 11. This is necessary for solving the governing equations by using V_{cell} instead of the potential at each electrode as the controlling variable. The equations at a given V_{cell} are solved by using the time-dependent solver (TBS), with the initial concentration profiles of various species as the initial inputting values. The time interval (Δt) between two iteration steps in a TBS solving task is adjusted according to the gap distance. Usually, a Δt value of $\tau/100$ ($\tau = L^2/4\pi D$) or smaller can give satisfactory results. We use Δt as small as 1×10^{-10} s for gaps of 10−100 nm width. The solving task is terminated when a steady-state current is obtained, which is indicated by a relative converging error of 0.001 or smaller between two adjacent iteration steps in a time period of *ca.* $\tau/4$.

Conflict of Interest: The authors declare no competing financial interest.

Acknowledgment. L. X. Fan, Y. W. Liu and S. L. Chen acknowledge the funding from the National Natural Science Foundation of China (Grant No. 21173162), the National Basic Research Program of China (Grant No. 2012CB932800), and the Hubei key Laboratory of Fuel Cell (Wuhan University of Technology). J. W. Xiong and H. S. White acknowledge the Office of Naval Research (USA).

REFERENCES AND NOTES

1. Anderson, L. B.; Reilley, C. N. Thin-Layer Electrochemistry: Use of Twin Working Electrodes for the Study of Chemical Kinetics. *J. Electroanal. Chem.* **1965**, *10*, 538–552.
2. Lewis, P. M.; Sheridan, L. B.; Gawley, R. E.; Fritsch, I. Signal Amplification in a Microchannel from Redox Cycling with Varied Electroactive Configurations of an Individually Addressable Microband Electrode Array. *Anal. Chem.* **2010**, *82*, 1659–1668.
3. Kätelhön, E.; Wolfrum, B. Simulation-Based Investigations on Noise Characteristics of Redox-Cycling Sensors. *Rev. Anal. Chem.* **2012**, *31*, 7–14.
4. Wolfrum, B.; Zevenbergen, M.; Lemay, S. Nanofluidic Redox Cycling Amplification for the Selective Detection of Catechol. *Anal. Chem.* **2008**, *80*, 972–977.
5. Bard, A. J.; Crayston, J. A.; Kittlesen, G. P.; Varco Shea, T.; Wrighton, M. S. Digital Simulation of the Measured Electrochemical Response of Reversible Redox Couples at Microelectrode Arrays: Consequences Arising from Closely Spaced Ultramicroelectrodes. *Anal. Chem.* **1986**, *58*, 2321–2331.
6. Goluch, E. D.; Wolfrum, B.; Singh, P. S.; Zevenbergen, M. A.; Lemay, S. G. Redox Cycling in Nanofluidic Channels Using Interdigitated Electrodes. *Anal. Bioanal. Chem.* **2009**, *394*, 447–456.
7. Li, T.; Hu, W.; Zhu, D. Nanogap Electrodes. *Adv. Mater.* **2010**, *22*, 286–300.
8. Rassaei, L.; Singh, P. S.; Lemay, S. G. Lithography-Based Nanoelectrochemistry. *Anal. Chem.* **2011**, *83*, 3974–3980.
9. Xiang, J.; Liu, B.; Wu, S. T.; Ren, B.; Yang, F. Z.; Mao, B. W.; Chow, Y. L.; Tian, Z. Q. Controllable Electrochemical Fabrication of Metallic Electrodes with a Nanometer/Angstrom-Sized Gap Using an Electric Double Layer as Feedback. *Angew. Chem., Int. Ed.* **2005**, *44*, 1265–1268.
10. Maljusch, A.; Nagaiah, T. C.; Schwamborn, S.; Bron, M.; Schuhmann, W. Pt-Ag Catalysts as Cathode Material for Oxygen-Depolarized Electrodes in Hydrochloric Acid Electrolysis. *Anal. Chem.* **2010**, *82*, 1890–1896.

11. Kätelhön, E.; Wolfrum, B. Simulation-Based Investigations on Noise Characteristics of Redox-Cycling Sensors. *Phys. Status Solidi A* **2012**, *209*, 881–884.
12. Singh, P. S.; Kätelhön, E.; Mathwig, K.; Wolfrum, B.; Lemay, S. G. Stochasticity in Single-Molecule Nanoelectrochemistry: Origins, Consequences, and Solutions. *ACS Nano* **2012**, *6*, 9662–9671.
13. Cutress, I. J.; Dickinson, E. J.; Compton, R. G. Electrochemical Random-Walk Theory: Probing Voltammetry with Small Numbers of Molecules: Stochastic *versus* Statistical (Fickian) Diffusion. *J. Electroanal. Chem.* **2011**, *655*, 1–8.
14. Suwatchara, D.; Henstridge, M. C.; Rees, N. V.; Compton, R. G. Experimental Comparison of the Marcus-Hush and Butler-Volmer Descriptions of Electrode Kinetics. The One-Electron Oxidation of 9,10-Diphenylanthracene and One-Electron Reduction of 2-Nitropropane Studied at High-Speed Channel Microband Electrodes. *J. Phys. Chem. C* **2011**, *115*, 14876–14882.
15. Zevenbergen, M. A.; Wolfrum, B. L.; Goluch, E. D.; Singh, P. S.; Lemay, S. G. Fast Electron-Transfer Kinetics Probed in Nanofluidic Channels. *J. Am. Chem. Soc.* **2009**, *131*, 11471–11477.
16. Batchelor-McAuley, C.; Dickinson, E. J.; Rees, N. V.; Toghill, K. E.; Compton, R. G. New Electrochemical Methods. *Anal. Chem.* **2011**, *84*, 669–684.
17. Bard, A. J.; Faulkner, L. R. Kinetics of Electrode Reactions. In *Electrochemical Methods: Fundamentals and Applications*; John Wiley & Sons: New York, 2001; pp 92−132.
18. Feldberg, S. W. Implications of Marcus−Hush Theory for Steady-State Heterogeneous Electron Transfer at an Inlaid Disk Electrode. *Anal. Chem.* **2010**, *82*, 5176–5183.
19. Liu, Y.; Chen, S. Theory of Interfacial Electron Transfer Kinetics at Nanometer-Sized Electrodes. *J. Phys. Chem. C* **2012**, *116*, 13594–13602.
20. Henstridge, M. C.; Ward, K. R.; Compton, R. G. The Marcus-Hush Model of Electrode Kinetics at a Single Nanoparticle. *J. Electroanal. Chem.* **2014**, *712*, 14–18.
21. Marcus, R. A. Chemical and Electrochemical Electron-Transfer Theory. *Annu. Rev. Phys. Chem.* **1964**, *15*, 155–196.
22. Hush, N. S. Adiabatic Rate Processes at Electrodes. I. Energy-Charge Relationships. *J. Chem. Phys.* **1958**, *28*, 962–972.
23. Hush, N. S. Electron Transfer in Retrospect and Prospect 1: Adiabatic Electrode Processes. *J. Electroanal. Chem.* **1999**, *470*, 170–195.
24. Chidsey, C. E. Free Energy and Temperature Dependence of Electron Transfer at the Metal-Electrolyte Interface. *Science* **1991**, *251*, 919–922.
25. Levich, V. G. In *Advances in Electrochemistry and Electrochemical Engineering*; Delahay, P., Tobias, C. W., Eds.; Interscience: New York, 1966; Vol. 4, p 249.
26. Gerischer, H. Electrochemical Techniques for the Study of Photosensitization. *Photochem. Photobiol.* **1972**, *16*, 243–260.
27. Norton, J. D.; White, H. S.; Feldberg, S. W. Effect of the Electrical Double Layer on Voltammetry at Microelectrodes. *J. Phys. Chem.* **1990**, *94*, 6772–6780.
28. Smith, C. P.; White, H. S. Theory of the Voltammetric Response of Electrodes of Submicron Dimensions. Violation of Electroneutrality in the Presence of Excess Supporting Electrolyte. *Anal. Chem.* **1993**, *65*, 3343–3353.
29. Dickinson, E. J.; Compton, R. G. Diffuse Double Layer at Nanoelectrodes. *J. Phys. Chem. C* **2009**, *113*, 17585–17589.
30. He, R.; Chen, S. L.; Yang, F.; Wu, B. L. Dynamic Diffuse Double-Layer Model for the Electrochemistry of Nanometer-Sized Electrodes. *J. Phys. Chem. B* **2006**, *110*, 3262–3270.
31. Chen, S. L.; Liu, Y. W. Electrochemistry at Nanometer-Sized Electrodes. *Phys. Chem. Chem. Phys.* **2014**, *16*, 635–652.
32. Fawcett, W. R. Examination of the Role of Ion Size in Determining Double Layer Properties on the Basis of a Generalized Mean Spherical Approximation. *J. Electroanal. Chem.* **2001**, *500*, 264–269.
33. Fawcett, W. R. Double Layer Effects in the Electrode Kinetics of Electron and Ion Transfer Reactions. In *Electrocatalysis*; Lipkowski, J., Ross, P. N., Eds.; Wiley-VCH: New York, 1998; p 322.
34. Oldham, K. B. Steady-State Voltammetry. In *Microelectrode: Theory and Application*; Montenegro, M. I., Queiros, M. A., Daschbach, J. L., Eds.; Kluwer: The Netherlands, 1991; pp 35−50.